



Hsa_circ_0001020 Serves as a Potential Biomarker for Gastric Cancer Screening and Prognosis

Jianing Yan^{1,2} · Yongfu Shao² · Haoxuan Lu¹ · Qihua Ye¹ · Guoliang Ye² · Junming Guo^{1,2}

Received: 7 January 2021 / Accepted: 2 August 2021 / Published online: 23 August 2021
© The Author(s), under exclusive licence to Springer Science+Business Media, LLC, part of Springer Nature 2021

Abstract

Circular RNAs (circRNAs) are an intriguing class of RNAs with covalently closed-loop structures. With characteristics of high stability and disease-specific expression, circRNAs are emerging as ideal targets for cancer therapy. However, the screening utility and clinical value of circRNAs in gastric cancer (GC) remain largely elusive. We detected levels of hsa_circ_0001020 in cell lines and tissue and plasma samples and investigated its clinicopathological correlations. Kaplan–Meier survival curves and regression analyses were used to analyze its prognostic value. Receiver operating characteristic curves and biomarker combinations were examined to verify its screening value. Bioinformatics analysis was also performed to predict potential biological functions. Our tests found that hsa_circ_0001020 was significantly upregulated in GC cell lines, GC tissue samples, and even in plasma. High hsa_circ_0001020 expression levels in GC tissues were significantly associated with distal metastasis and blood carbohydrate antigen 19-9 (CA19-9). GC patients with high hsa_circ_0001020 had a lower overall survival and disease-free survival time than the low levels. Regression analysis suggested that the level of hsa_circ_0001020 expression was an independent prognostic factor for survival time. As a biomarker for GC, hsa_circ_0001020 showed a superior AUC, sensitivity, and specificity than carcinoembryonic antigen and CA19-9, and was suitable for combination with clinical tumor biomarkers. Bioinformatics analysis provided valuable clues for the possible oncogenic pathways of GC, such as the FoxO and *p53* signaling pathways. In conclusion, our study found that hsa_circ_0001020 in GC could be a reliable biomarker to screen for GC and predict prognosis.

Keywords Circular RNA · Hsa_circ_0001020 · Biomarker · Gastric cancer · Prognosis

Introduction

Worldwide, gastric cancer (GC) is one of the most common malignancies. Recent studies have revealed that it is the fourth leading cause of cancer-related mortality worldwide [1]. Despite recent developments in therapy, only a small proportion of patients obtain an accurate diagnosis in the early stage of GC, leading to a low survival rate in

Asia [2]. Unfortunately, current traditional tumor biomarkers, such as carbohydrate antigen 19-9 (CA19-9), CA72-4, and carcinoembryonic antigen (CEA), show a low positivity rate in GC screening [3]. Lacking clear metrics, clinicians are unable to develop appropriate treatments for individual patients. Thus, it is necessary to find novel noninvasive biomarkers for GC screening.

Circular RNA (circRNA), produced by the alternative splicing of precursor RNA, is an intriguing class of RNA with a covalently closed-loop structure that has attracted increasing attention because of its characteristics of cellular abundance, biological function, and high stability [4, 5]. Moreover, circRNAs are also involved in regulating several biological functions, such as proliferation, metastasis, and apoptosis [6, 7]. Furthermore, circRNAs can be stably detected in the blood, so they have been reported to be screening biomarkers and even potential therapeutic targets for multiple tumors [8, 9].

✉ Guoliang Ye
ndfyyl@126.com

Junming Guo
guojunming@nbu.edu.cn

¹ Department of Biochemistry and Molecular Biology and Zhejiang Key Laboratory of Pathophysiology, Ningbo University School of Medicine, Ningbo 315211, China

² Department of Gastroenterology, The Affiliated Hospital of Medical School of Ningbo University, Ningbo 315020, China

Hsa_circ_0001020 is a dysregulated circRNA in GC that has been analyzed with circRNA microarrays and can also be searched in circBase (<http://www.circbase.org>). It is encoded by UDP-glucose pyrophosphorylase 2 (*UGP2*), located at chr2:64,083,439–64,085,070, and has 1631 nucleotides. However, no databases have reported the hsa_circ_0001020 expression level and clinical significance in GC. Hence, we detected the level of hsa_circ_0001020 in GC cell lines, GC tissues, and plasma. Moreover, clinicopathological factors were examined, and receiver operating characteristic (ROC) curves and Kaplan–Meier survival curves were generated to analyze its screening and prognostic values. A linear regression analysis model and multivariate Cox regression model were built to examine its prognostic value. Finally, bioinformatics analysis was performed to predict the biological functions of hsa_circ_0001020. Our results demonstrated that the upregulation of hsa_circ_0001020 can serve as a potential biomarker for gastric cancer screening and prognosis.

Materials and Methods

Specimens and Clinical Information

Tissue samples and plasma were obtained from the Cancer Center for Gastroenterology, the Affiliated Hospital of the Medical School of Ningbo University, China, between 2012 and 2017. Cancer tissues and paired adjacent nontumorous tissues (5 cm from the edge of the tumor) were collected from 63 patients who underwent surgical procedures. Furthermore, 61 healthy gastric mucosa and 61 gastritis and 30 gastric intestinal metaplasia (GIM) samples were collected as biopsy specimens. Sixty-two GC patient plasma samples before and 2 weeks after surgery and 46 healthy plasma samples were obtained. Tissue samples were immediately immersed in RNA fixer (Biotek, Beijing, China) after removal and preserved at -80°C for further use. This study was approved by the Human Research Ethics Committee of Ningbo University (IRB No. 20120303).

Tumor clinical stages and histological grades were assessed according to the Tumor-Node-Metastasis (TNM) staging system (8th ed) and National Comprehensive Cancer Network clinical practice guidelines of oncology (V.1.2012), respectively. Each selected patient provided written informed consent prior to gastroscopy, and all experimental protocols in this study were approved by the Ethics Committee of Ningbo University School of Medicine (No. 2017022701).

Cell Culture

Three human GC cell lines (BGC-823, AGS, and SGC-7901) and the normal human gastric epithelial cell line (GES-1) were obtained from the Shanghai Institute of Biochemistry

and Cell Biology, Chinese Academy of Sciences, China. All cell lines were cultured in RPMI-1640 medium (Life Technologies, Grand Island, NY, USA) with 10% fetal bovine serum.

RNA Isolation and Reverse Transcription

RNA was extracted from tissue and plasma using TRIzol reagents and TRIzol LS reagents (Ambion, Carlsbad, CA, USA), respectively. Subsequently, total RNA was used as a template and reverse transcribed to cDNA using a GoScript Reverse Transcription (RT) System (Promega, Madison, WI, USA) according to the manufacturer's instructions [10]. cDNA samples were stored at -80°C for further use.

Quantitative Real Time RT-Polymerase Analysis (qRT-PCR)

qRT-PCR was performed with GoTaq qPCR Master Mix (Promega) according to the manufacturer's instructions on an Mx3005P Real-Time PCR System (Stratagene, La Jolla, CA, USA). The reaction conditions were as follows: denaturation at 95°C for 15 s, annealing at 53°C for 30 s, and extension at 72°C for 30 s for 40 cycles, and then extension at 72°C for 7 min. Glyceraldehyde 3-phosphate dehydrogenase (GAPDH) was served as the reference for hsa_circ_0001020. and a lower ΔCt value indicated higher expression. Results from at least two independent experiments were averaged and were presented as the mean \pm SD (standard deviation). The sequences of primers were as follows: 5'-GCCTTCTGTGGATTGGGGAA-3' and 5'-AGC TCTTGCCGAATGACTTCT-3' for hsa_circ_0001020, and 5'-ACCCACTCCTCCACCTTTGAC-3' (sense) and 5'-TGT TGCTGTAGCCAAATTCGTT-3' (antisense) for GAPDH. Both primers were synthesized by BGI Group (Guangdong, China). The ΔCt method was used to normalize levels of circRNA. Hsa_circ_0001020 levels were calculated using the ΔCt method ($\Delta\text{Ct} = \text{Ct}_{\text{hsa_circ_0001020}} - \text{Ct}_{\text{GAPDH}}$). A higher ΔCt was indicative of a lower hsa_circ_0001020 level. The $\Delta\Delta\text{Ct}$ method ($\Delta\Delta\text{Ct} = \Delta\text{Ct}_{\text{GC cell}} - \Delta\text{Ct}_{\text{GES-1}}$) was used to compare hsa_circ_0001020 levels in GC cell lines for calculating relative expression [11]. A higher $2^{-\Delta\Delta\text{Ct}}$ value indicates a higher expression level in relative expression.

Prediction of Hsa_circ_0001020/miRNA Interactions

Hsa_circ_0001020/miRNA interactions were predicted and annotated via Arraystar's homemade miRNA target prediction software based on TargetScan and miRanda [12]. Then, Gene Ontology (GO) annotation and Kyoto Encyclopedia of Genes and Genomes (KEGG) pathway analysis were performed [13]. The interaction network of hsa_circ_0001020/miRNA pathways was constructed with Cytoscape Software

(<https://cytoscape.org>). A Venn diagram was constructed with Venny 2.1 software (<http://bioinfogp.cnb.csic.es/tools/venny/>).

Statistical Analysis

SPSS v.22.0 for Windows (SPSS, Chicago, IL, USA) and GraphPad Prism 8.0 (GraphPad Software, USA) were used for data processing and graph generation. Student's *t* test and one-way analysis of variance (ANOVA) were used for comparisons, as appropriate. Linear regression analysis and multivariate Cox logistic regression were performed to identify factors influencing survival time and confirm the association between the outcome and the expression of hsa_circ_0001020. ROC and Kaplan–Meier survival plots were generated to evaluate prognostic values. $P < 0.05$ was deemed statistically significant.

Results

Profiling the Expression of Hsa_circ_0001020 in GC

All GC cells exhibited higher expression levels hsa_circ_0001020 than GES-1 cells (Fig. 1a). Compared with their paired adjacent nontumorous tissues, hsa_circ_0001020 was also upregulated in gastric cancer tissue (Fig. 1b). Hsa_circ_0001020 was significantly upregulated in 63.49% (40/63) of GC tissues. Similarly, compared with tissue from other pathological changes, its expression level was remarkably increased in cancer tissue (Fig. 1c). There was no significant difference between the healthy and gastritis groups.

Moreover, an ROC curve was generated to determine the potential diagnostic value of hsa_circ_0001020. The area under the ROC curve (AUC) was 0.702 (95% confidence interval [CI], 0.614–0.781; $P < 0.001$). The cutoff value, sensitivity and specificity were 8.375, 73.02%, and 62.3%, respectively, at the maximum of Youden index (Fig. 1d).

Upregulated Hsa_circ_0001020 Expression Is Associated with Clinicopathological Characteristics in GC Patients

We collected and summarized the clinicopathological information of the 63 GC patients in Table 1. The data suggested that the hsa_circ_0001020 expression level was significantly associated with distal metastasis ($P = 0.014$). Furthermore, our analysis suggested that hsa_circ_0001020 expression in tissue was also significantly correlated with blood CA19-9 (Fig. 2, $P = 0.0119$).

The Prognostic Value of Hsa_circ_0001020 in GC

To better understand the potential prognostic roles of hsa_circ_0001020 in GC, GC patients were classified into high and low expression groups. The $\Delta\Delta Ct$ method ($\Delta\Delta Ct = \Delta Ct_{GC\ tissue} - \Delta Ct_{adjacent\ nontumorous\ tissues}$) was used to compare hsa_circ_0001020 levels in GC tissues and paired adjacent nontumorous tissues. Patients whose $\Delta\Delta Ct$ was greater than 0 were placed into the high group, and those with values less than 0 were placed in the low group. Moreover, the difference in hsa_circ_0001020 levels between matching samples was analyzed by the $2^{-\Delta\Delta Ct}$ method, and an amount greater than 1 meant that hsa_circ_0001020 was much higher in GC tissues. The low expression group had obviously longer overall survival (Fig. 1e; $P = 0.0213$) and disease-free survival times (Fig. 1f; $P = 0.0206$).

Tables 2 and 3 show the multivariate analysis of clinicopathological factors related to patient prognosis. Multivariate regression analysis showed that the hsa_circ_0001020 expression level was an independent prognostic factor for disease-free survival (HR = 1.539, 95% CI 1.140–2.078; $P = 0.005$). The level of hsa_circ_0001020 expression (X1) and tumor diameter (X2, centimeters) were influencing factors of overall and disease-free survival time (Y, months). The regression function is as follows (Tables 4, 5):

$$Y(\text{Overall}) = 55.822 - 2.989 \times X1 - 1.977 \times X2$$

$$Y(\text{Disease-free}) = 55.422 - 3.743 \times X1 - 1.77 \times X2$$

Plasma Hsa_circ_0001020 Is a Screening Biomarker for GC

Because of the complicated composition of the plasma, we first evaluated our products and confirmed that hsa_circ_0001020 existed in plasma, and that the sequences were consistent with that in the circBase database (<http://circbase.org/>), as expected Fig. 3a). Furthermore, we analyzed our samples from preoperative and postoperative (2 weeks) GC patients as well as healthy volunteers. Our analysis showed that hsa_circ_0001020 was downregulated in the postoperative ($P < 0.05$) and healthy groups ($P < 0.001$; Fig. 3b, c). All plasma samples were analyzed in duplicate to provide more precise measurements.

An ROC curve was constructed to determine the potential screening value of hsa_circ_0001020 in plasma. The AUC was 0.738 (95% CI 0.642–0.819; $P < 0.001$). The cutoff value, sensitivity, and specificity were 3.355, 46.55%, and 97.83%, respectively, at the maximum of Youden index (Fig. 3d). When CEA and CA19-9 were combined as plasma biomarkers with hsa_circ_0001020, the AUC, sensitivity and specificity were 0.852 (95% CI 0.767–0.915; $P < 0.001$), 68.5%, and 89.1%, respectively, almost agreeing with the combined use of only CEA and hsa_circ_0001020 (0.852, 66.7%, and 91.3%; Fig. 3e). In the heat map, we

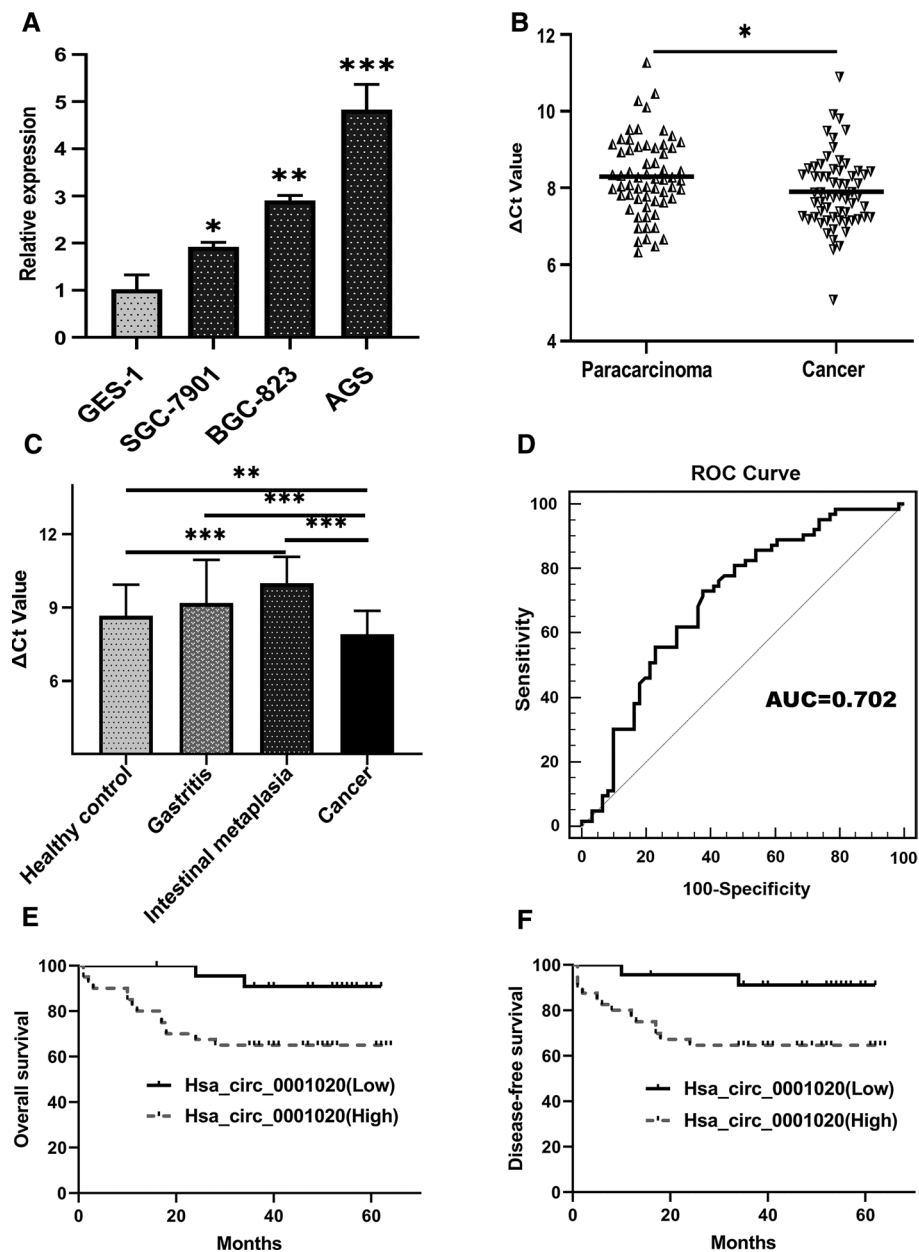


Fig. 1 Hsa_circ_0001020 expression levels in gastric cancer tissues and cell lines. **a** Relative expression of has_circ_0001020 in three gastric cancer cell lines and a normal gastric epithelial cell line GES-1. Data are presented as the mean \pm SD. Compared with GES-1, hsa_circ_0001020 was upregulated in three GC cell lines (SGC-7901, BGC-823, and AGS). **b** Hsa_circ_0001020 expression levels were increased in GC tissues ($n = 63$). Hsa_circ_0001020 was upregulated in 63.49% (40/63) of gastric cancer tissues. **c** Hsa_circ_0001020 levels in healthy controls ($n = 61$), gastritis patients ($n = 61$), dysplasia patients ($n = 30$), and gastric cancer patients ($n = 63$). Hsa_circ_0001020 was remarkably increased in gastric can-

cer patients compared with the healthy individuals. Compared with that in the healthy group, the expression in the intestinal metaplasia group was significantly decreased. **d** ROC curve of hsa_circ_0001020 for distinguishing gastric cancer tissues from adjacent normal tissues. The AUC was 0.702 (95% confidence interval [CI], 0.614–0.781; $P < 0.001$). The cutoff value, sensitivity and specificity were 8.375, 73.02% and 62.3%, respectively. **e** Kaplan–Meier analysis of hsa_circ_0001020 expression levels and overall survival. **f** Kaplan–Meier analysis of hsa_circ_0001020 expression levels and disease-free survival. (* $P < 0.05$, ** $P < 0.01$, *** $P < 0.001$)

listed all possible combinations of four types of biomarkers to identify the most effective combination for the diagnosis for gastric cancer. The obtained AUC, sensitivity, and specificity are shown in Fig. 3f.

Annotation of Hsa_circ_0001020 Function

It was predicted that hsa_circ_0001020 could harbor hsa-miR-19a-3p and hsa-miR-103a-2-5p binding sites by

Table 1 Correlation between hsa_circ_0001020 expression levels in gastric cancer tissues (ΔCt) and clinicopathological parameters of patients with gastric cancer

Characteristics	No. of cases (%)	Mean \pm SD	<i>P</i> value
Age (years)			
≥ 60	42 (66.7)	7.9437 \pm 1.084	0.671
< 60	21 (33.3)	7.8345 \pm 0.615	
Sex			
Male	44 (69.8)	7.8117 \pm 0.773	0.227
Female	19 (30.2)	8.1287 \pm 1.266	
Tumor location			
Sinuses ventriculi	28 (44.4)	7.9667 \pm 0.974	0.759
Cardia	17 (27.0)	7.7591 \pm 1.053	
Others	18 (28.6)	7.9550 \pm 0.841	
Diameter (cm)			
≥ 5	33 (52.4)	8.0014 \pm 1.026	0.414
< 5	30 (47.6)	7.8038 \pm 0.863	
Differentiation			
Poor	32 (50.8)	7.7009 \pm 0.941	0.209
Moderate	26 (41.3)	8.1408 \pm 0.923	
Well	5 (7.9)	8.0140 \pm 1.036	
TNM stage			
Early	16 (25.4)	8.2425 \pm 1.115	0.102
Advanced	47 (74.6)	7.7932 \pm 0.870	
Borrmann’s type			
I & II	9 (19.1)	7.3589 \pm 1.110	0.096
III & IV	38 (80.9)	7.8961 \pm 0.786	
Lauren’s type			
Intestinal	25 (39.7)	8.088 \pm 1.011	0.223
Diffuse and mixed	38 (60.3)	7.788 \pm 0.900	
Pathologic diagnosis			
Signet ring cell cancer	11 (17.5)	7.5436 \pm 1.034	0.164
Adenocarcinoma	52 (82.5)	7.9842 \pm 0.923	
Invasion			
T ₁ and T ₂	20 (31.7)	8.2310 \pm 1.000	0.064
T ₃ and T ₄	43 (68.3)	7.7567 \pm 0.897	
Lymphatic metastasis			
N ₀	23 (36.5)	7.9965 \pm 0.764	0.576
N ₁₋₃	40 (63.5)	7.8560 \pm 1.047	
Distal metastasis			
M ₀	43 (68.3)	8.1059 \pm 0.926	0.014
M ₁	20 (31.7)	7.4803 \pm 0.873	
Venous invasion			
Absent	30 (47.6)	7.8042 \pm 0.824	0.415
Present	33 (52.4)	8.0011 \pm 1.054	
Perineural invasion (PNI)			
Absent	29 (46.0)	8.0136 \pm 1.034	0.416
Present	34 (54.0)	7.8166 \pm 0.876	
CEA (tissue)			
Positive	54 (85.7)	7.9140 \pm 0.957	0.892
Negative	9 (14.3)	7.8672 \pm 0.955	

Table 1 (continued)

Characteristics	No. of cases (%)	Mean \pm SD	<i>P</i> value
CA19-9 (tissue)			
Positive	29 (54)	7.9555 \pm 1.049	0.713
Negative	34 (46)	7.8662 \pm 0.869	

The bold values indicate data are of statistical significance

miRNA seed sequence matching (Fig. 4a). A network, consisting of hsa-miR-19a-3p and hsa-miR-103a-2-5p with their target transcripts (Fig. 4b), was generated using Cytoscape software. A Venn diagram identified 159 common target genes of both miRNAs (Fig. 4c). In light of the targeted genes, GO and KEGG pathway analyses helped elucidate that they were involved in regulating multiple biological processes and signaling pathways, such as gene expression and the FoxO and p53 signaling pathways (Fig. 4d, e).

Discussion

There are two critical obstacles to the long-term survival of patients with cancer. One is that there are no satisfactory markers to identify early-stage cancers in asymptomatic individuals, or to differentiate benign from malignant disease. Additionally, there are no methods to monitor and intervene with dynamic changes that occur during or after therapy.

CircRNAs are considered critical regulators of gene expression and are becoming an emerging hotspot in oncologic biomarker research because of their conserved, stable character and tissue, time, and disease specificity [14]. An increasing number of studies have reported that circRNAs are abnormally expressed in tumor cells and tissues [15]. For example, in hepatocellular carcinoma (HCC), circRNA_101237 was determined to be upregulated in tumor tissue, providing novel insights into HCC therapy [16]. In addition, circRNAs have shown strong associations with clinicopathological features in GC. The downregulation of hsa_circ_0005556 was remarkably correlated with TNM stage, differentiation, and lymphatic metastasis [17]. Moreover, the dysregulation of circ-CCDC66 in both colorectal cancer tissues and plasma was predicted to be an indicator for diagnostic evaluation [18]. All these results indicate that circRNAs have promise as novel screening and prognostic biomarkers.

Mechanistically, GC involves multiple steps and multiple factors, and originates from conditions such as inflammation to atrophic gastritis, GIM, and ultimately to adenocarcinoma, where GIM is a key and premalignant stage [19, 20]. Our analysis first showed that hsa_circ_0001020 was remarkably upregulated in GC cell lines and tissues (Fig. 1).

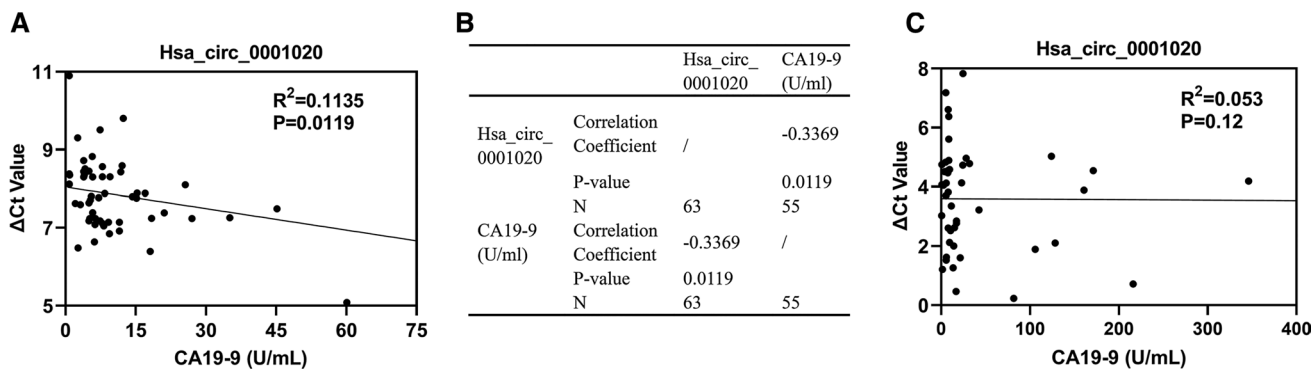


Fig. 2 The correlation of hsa_circ_0001020 with gastric cancer clinical characteristics. **a** Curve regression analysis of CA19-9 and hsa_circ_0001020 in gastric cancer tissues. **b** Spearman correlation

analysis of CA19-9 and hsa_circ_0001020 in gastric cancer tissues. **c** Curve regression analysis of CA19-9 and hsa_circ_0001200 in gastric cancer plasma

Table 2 Cox regression analysis of overall survival time

Clinical variable	Univariate analysis		Multivariate analysis	
	Hazard ratio (95% CI)	P value	Hazard ratio (95% CI)	P value
Sex	0.597	0.642		
Age	1.073	0.232		
Blood CEA	1.009	0.805		
Blood CA19-9	1.000	0.965		
Borrmann’s type	11.238	0.121		
Lauren’s type	5.701	0.418		
Distal metastasis	1177.086	0.012	20.502	0.015
Venous invasion	0.434	0.527		
Lymphatic metastasis	179.014	0.110		
Perineural invasion	0.642	0.685		
Differentiation	0.147	0.355		
Diameter	1.188	0.454		
TNM stage	0.005	0.030		
Hsa_circ_0001020 expression (2 ^{-ΔΔCt} method)	1.673	0.196		
Recurrence	32.167	0.002	23.623	< 0.001

Entry 0.05; Removal: 0.1 P = 0.008

The bold values indicate data are of statistical significance

Table 3 Cox regression analysis of disease-free survival time

Clinical variable	Univariate analysis		Multivariate analysis	
	Hazard ratio (95% C.I.)	P value	Hazard ratio (95% C.I.)	P value
Sex	1.885	0.515		
Age	0.994	0.909		
Blood CEA	1.045	0.171		
Blood CA19-9	0.996	0.385		
Borrmann’s type	0.781	0.857		
Lauren’s type	41.152	0.080		
Distal metastasis	713.395	0.071		
Venous invasion	0.391	0.381		
Lymphatic metastasis	90.887	0.193		
Perineural invasion	1.378	0.742		
Differentiation	0.065	0.120		
Diameter	1.857	0.012	1.290	0.062
TNM stage	0.006	0.087		
Hsa_circ_0001020 expression (2 ^{-ΔΔCt} method)	1.994	0.085	1.319	0.01

Entry 0.05; Removal: 0.1, P = 0.006

The bold values indicate data are of statistical significance

Then, we expanded the scope and the amounts of the samples. In each pathological process, we found that the hsa_circ_0001020 expression level was prominently increased in cancer tissue and lowest in GIM (Fig. 1). Goblet cells, which are lacking in healthy gastric mucosa, are distinctively present and are pathognomonic for GIM. Hence, we hypothesize that GIM has more goblet cells and fewer parietal cells that secrete less hsa_circ_0001020 than healthy tissue. To date, the change trends of hsa_circ_0001020 in cell and tissue lines show consistent elevation.

It has been reported that clinicopathologic features are independent prognostic factors of GC [21], in which peritoneal metastasis is the most important factor for prognosis in GC and essential for selecting an effective treatment strategy [22]. Interestingly, hsa_circ_0001020 not only correlated positively with distal metastasis but also showed a positive correlation with CA19-9 (Table 1; Fig. 2), which meant that patients with high hsa_circ_0001020 had a worse prognosis. Moreover, patients with higher hsa_circ_0001020 had lower overall and disease-free survival times (Fig. 1). In line with this observation, we performed Cox regression analysis to identify additional related factors, and our results showed

Table 4 Multiple linear regression analysis of overall survival time

Model	Unstandardized coefficients		Standardized coefficients		95% CI
	Beta	Std. Error	Beta	P value	
Constant	56.207	4.81			46.578–65.836
Hsa_circ_0001020 Expression (X1) (2 ^{-ΔΔCt} method)	-3.163	1.13	-0.331	0.007	-5.426 to -0.900
Diameter (X2)	-1.97	0.7	-0.333	0.007	-3.371 to -0.568

Entry 0.1; Removal: 0.15, *P* = 0.002
 $Y(\text{time}) = 56.207 - 3.163 \times X1 - 1.97 \times X2$

Table 5 Multiple linear regression analysis of disease-free survival time

Model	Unstandardized coefficients		Standardized coefficients		95% CI
	Beta	Std. Error	Beta	P value	
Constant	55.72	5.351			44.997 to 66.443
Hsa_circ_0001020 Expression (X1) (2 ^{-ΔΔCt} method)	-3.813	1.258	-0.373	0.04	-6.334 to -1.291
Diameter (X2)	-1.791	0.803	-0.274	0.03	-3.4 to -0.182

Entry 0.1; Removal: 0.15; *P* = 0.004
 $Y(\text{time}) = 55.72 - 3.813 \times X1 - 1.791 \times X2$

that the hsa_circ_0001020 level was an independent negative prognostic factor for disease-free survival (Table 3). This is why we hypothesized that the expression of hsa_circ_0001020 may be associated with the recurrence of GC. Furthermore, we performed linear regression analysis and revealed a negative relationship between hsa_circ_0001020 expression and survival time (Tables 4, 5). All this evidence suggests that hsa_circ_0001020 is closely correlated with GC and plays a critical role in GC clinical progression and prognosis.

Due to the unsatisfactory sensitivity or specificity of the existing blood indicators of GC, a panel approach of biomarker combinations will enable us to conduct more accurate screening. CircRNAs can be stable and detectable in blood, so an increasing number of circRNAs appear to be ideal indicators for cancer screening [23–25]. Nevertheless, it has been confirmed that this change does not occur after chemoradiation because cancer cells secrete membrane vesicles containing tumor-derived mutant RNA, and the level of release might decrease only after excision [26, 27]. Consistently, hsa_circ_0001020 was upregulated in GC plasma, and, more importantly, the level of hsa_circ_0001020 was remarkably downregulated 2 weeks after surgical resection compared to preoperatively (Fig. 3b). Additionally, as a single biomarker, plasma hsa_circ_0001020 had a higher AUC value (0.738) than CEA (0.560) and CA72-4 (0.670) [28], whose sensitivity was 46.55%, much better than traditional markers such as CEA (21.1%), CA19-9 (27.8%), and CA72-4 (30.0%) to

screen gastric cancer [3]. Furthermore, we investigated and reported the results of combinations of three biomarkers. When CEA, CA19-9 and hsa_circ_0001020 were combined, the AUC, sensitivity, and specificity were 0.852, 68.5%, and 89.1%, respectively (Fig. 3f). More interestingly, combining only CEA and hsa_circ_0001020 significantly improved the sensitivity and specificity, to 66.7% and 91.3%, respectively, which deserves further study in larger patient cohorts to validate our results. Overall, hsa_circ_0001020 is simultaneously upregulated in GC cell, tissue as well as plasma, which can be reliable in screening GC and can help to monitor recurrence after surgery.

Mechanistically, a variety of circRNAs regulate gene expression by functioning as miRNA sponge molecules [29], and the circRNA-miRNA-target gene pathway plays vital roles in cancer cell initiation, cell proliferation, apoptosis, angiogenesis, invasion, metastasis, and drug resistance [30]. Qu et al. identified that circFLNA acted as a sponge of miR-646 [31]. Li et al. demonstrated that circ0001017 suppressed gastric cancer progression by modulating the miR-197/RHOB signaling pathway [32]. We found that hsa_circ_0001020 harbors hsa-miR-19a-3p and hsa-miR-103a-2-5p binding sites (Fig. 4), and that these two miRNAs participate in the majority of pathways of cancer, such as the p53 and FoxO signaling pathways, apoptosis, cell cycle, and transcriptional dysregulation, which may be relevant in our follow-up study and provide some clues for possible oncogenic pathways of GC.

In conclusion, our study found that hsa_circ_0001020 in GC is a novel and practical biomarker for screening and prognostic estimation.

Fig. 3 Hsa_circ_0001020 as a screening biomarker for gastric cancer. **a** The results of amplified products in GC plasma validated the back-splice junction sequences of hsa_circ_0001020 by DNA sequencing. **b** Detection of hsa_circ_0001020 levels in human GC plasma before and 2 weeks after surgery ($n = 62$). **c** Detection of hsa_circ_0001020 levels in human GC plasma ($n = 62$) and healthy controls ($n = 46$). **d** ROC curve of hsa_circ_0001020 in preoperative gastric cancer plasma and the healthy. The AUC was 0.738 (95% CI, 0.642–0.819; $P < 0.001$). The cutoff value, sensitivity, and specificity were 3.355, 46.55%, and 97.83%, respectively. **e** Pairwise comparison of the diagnostic values of plasma hsa_circ_0001020, blood CEA and blood CA19-9. When CEA, CA19-9 and hsa_circ_0001020 were combined, the AUC, sensitivity and specificity were 0.852 (95% CI, 0.767–0.915; $P < 0.001$), 68.5%, and 89.1%, respectively. **f** The obtained AUC and the corresponding specificity and sensitivity are shown on the heat map ($*P < 0.05$, $***P < 0.001$)

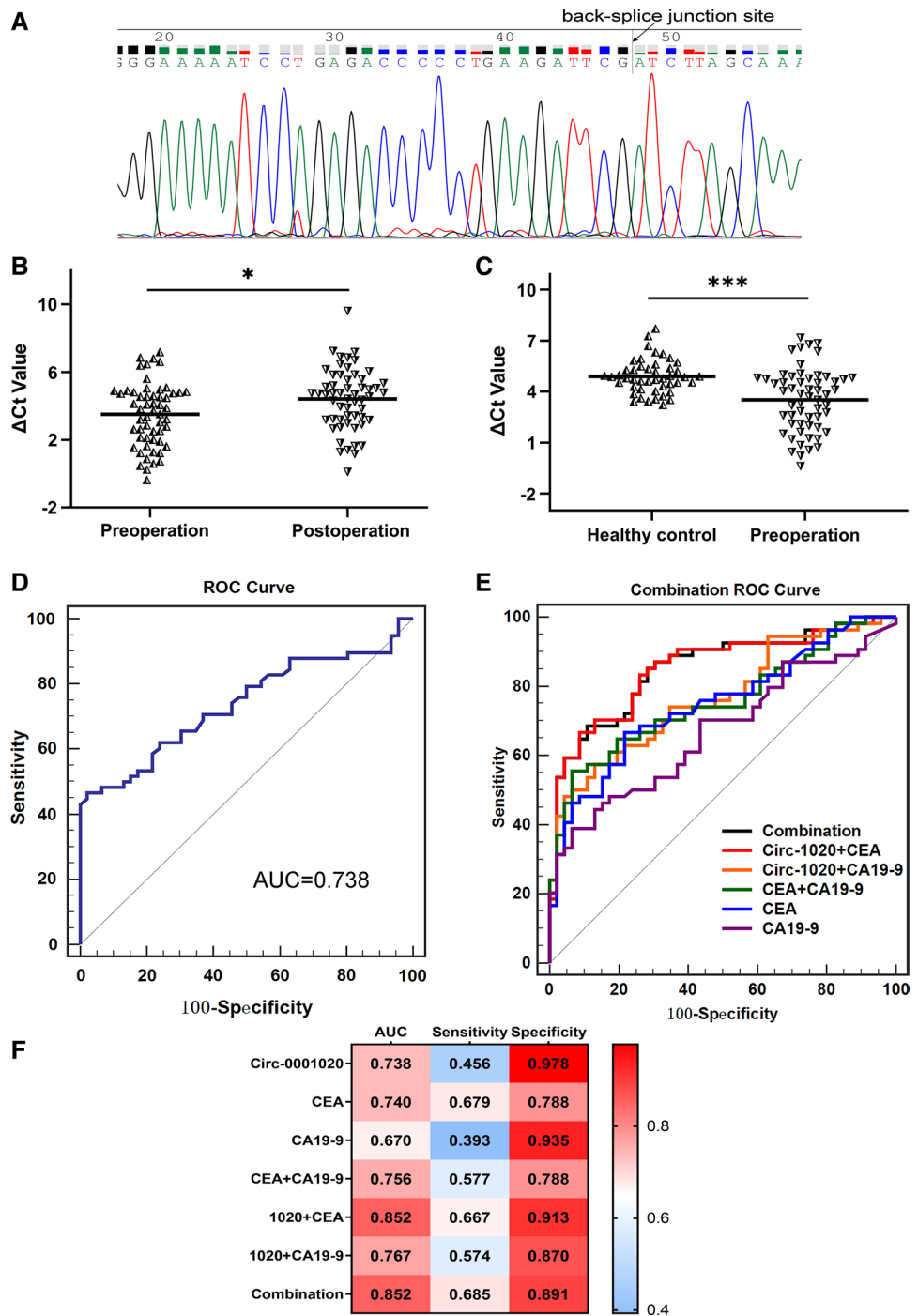
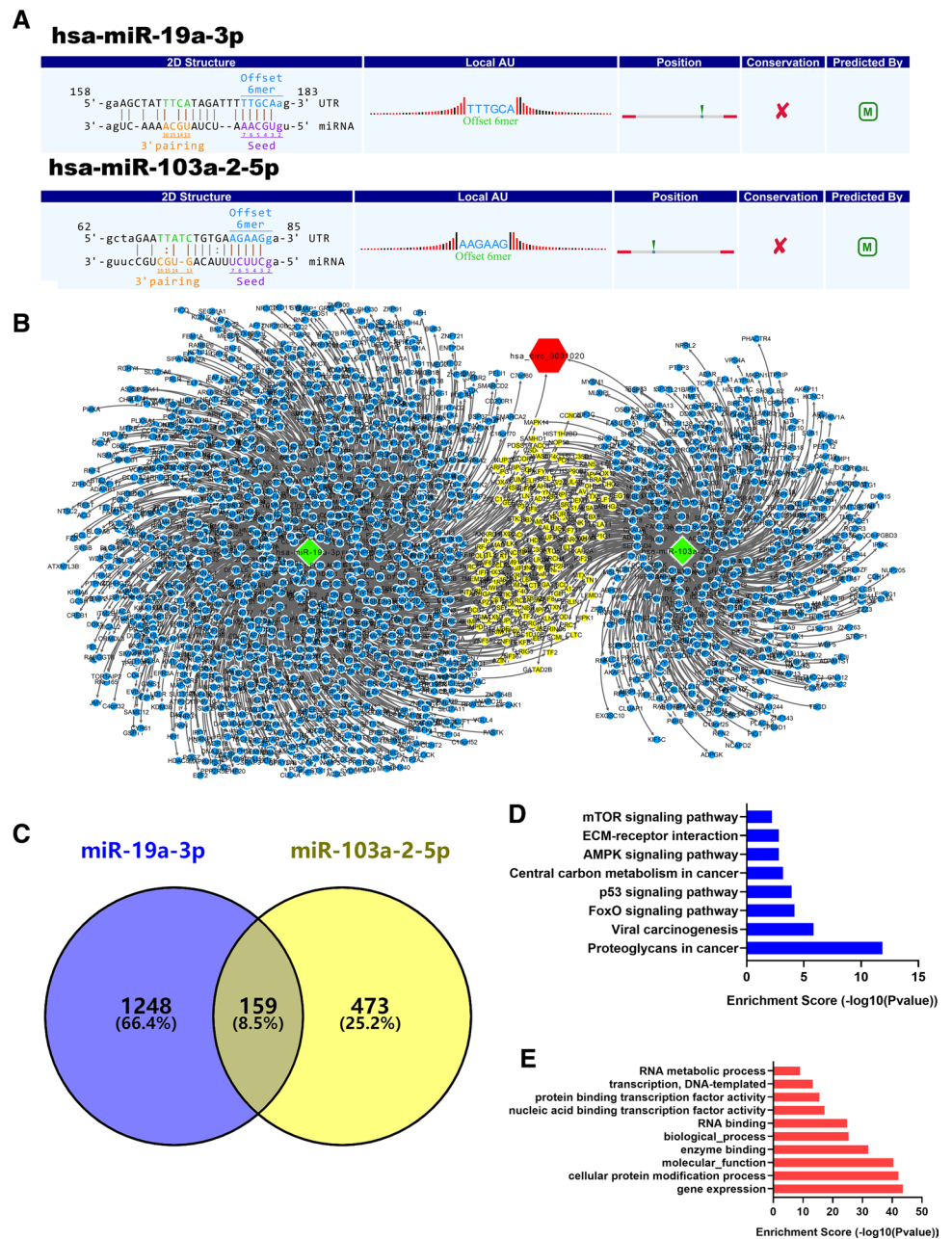


Fig. 4 Prediction of hsa_circ_0001020/microRNA interactions and related pathways. **a** Prediction of hsa_circ_0001020/miRNA interactions based on TargetScan and miRanda. **b** The interaction network map of hsa_circ_0001020-miRNA-target genes (hsa_circ_0001020: *red hexagon*; hsa-miR-19a-3p and hsa-miR-103a-2-5: *green diamond*; target genes: *blue node*; and MYC: *yellow node*). **c** Venn diagram showing common targets of hsa-miR-19a-3p and hsa-miR-103a-2-5. **d** Hsa_circ_0001020-miRNA KEGG analysis. **e** Hsa_circ_0001020-miRNA GO analysis



Acknowledgments This work was supported by the National Natural Science Foundation of China (Nos. 81702367, 81772279), the Medical and Health Research Project of Zhejiang Province (No. 2018KY159), the Affiliated Hospital of Medical School of Ningbo University Youth Talent Cultivation Program (No. FYQMKY202001) and the Scientific Research Foundation of Graduate School of Ningbo University (No. IF2020160).

Declarations

Conflict of interest The authors declare no potential conflicts of interests.

References

- Sung H, Ferlay J, Siegel RL, et al. Global Cancer Statistics 2020: GLOBOCAN Estimates of Incidence and Mortality Worldwide for 36 Cancers in 185 Countries *CA Cancer J Clin*. 2021;71:209-249.
- Wang Y, Li Z, Xu S, et al. Novel potential tumor biomarkers: Circular RNAs and exosomal circular RNAs in gastrointestinal malignancies. *J Clin Lab Anal*. 2020;34:e23359.
- Shimada H, Noie T, Ohashi M, et al. Clinical significance of serum tumor markers for gastric cancer: a systematic review of literature by the Task Force of the Japanese Gastric Cancer Association. *Gastric Cancer*. 2014;17:26-33.
- Yan L, Chen Y. Circular RNAs in immune response and viral infection. *Trends Biochem Sci*. 2020;45:1022-1034.

5. Ruan Y, Li Z, Shen Y, et al. Functions of circular RNAs and their potential applications in gastric cancer. *Expert Rev Gastroenterol Hepatol*. 2020;14(2):85-92.
6. Pinelopi I Artemaki, Andreas Scorilas, Christos K Kontos, Circular RNAs: A new piece in the colorectal cancer puzzle. *Cancers*. 2020;12:2464.
7. Sun R, Li H, Li J, et al. CircRNA circ-0038718 promotes hepatocellular carcinoma progression through sponging miR-139-3p. *Biochem Biophys Res Commun*. 2020;533:845-852.
8. Zhang H, Shen Y, Li Z, et al. The biogenesis and biological functions of circular RNAs and their molecular diagnostic values in cancers. *J Clin Lab Anal*. 2020;34(1):e23049.
9. Li F, Huang Q, Gong Z, et al. Diagnostic and prognostic roles of circ-SHPRH for solid cancers: a meta-analysis. *Onco Targets Ther*. 2019;12:4351-4357.
10. Shao Y, Li J, Lu R, et al. Global circular RNA expression profile of human gastric cancer and its clinical significance. *Cancer Med*. 2017;6:1173-1180.
11. Shao Y, Tao X, Lu R, et al. Hsa_circ_0065149 is an indicator for early gastric cancer screening and prognosis prediction. *Pathol Oncol Res*. 2020;26:1475-1482.
12. Wu G, Zhou W, Lin X, et al. circRASSF2 acts as ceRNA and promotes papillary thyroid carcinoma progression through miR-1178/TLR4 signaling pathway. *Mol Ther Nucleic Acids*. 2020;19:1153-1163.
13. Lee WH, Tsai MJ, Chang WA, et al. Deduction of novel genes potentially involved in hypoxic AC16 human cardiomyocytes using next-generation sequencing and bioinformatics approaches. *Int J Mol Med*. 2018;42:2489-2502.
14. Yu X, Ding H, Yang L, et al. Reduced expression of circRNA hsa_circ_0067582 in human gastric cancer and its potential diagnostic values. *J Clin Lab Anal*. 2020;34:e23080.
15. Lu J, Zhang P, Xie J, et al. Hsa_circ_0000467 promotes cancer progression and serves as a diagnostic and prognostic biomarker for gastric cancer. *J Clin Lab Anal*. 2019;33:e22726.
16. Zhou S, Wei J, Wang Y, et al. Cisplatin resistance-associated circRNA_101237 serves as a prognostic biomarker in hepatocellular carcinoma. *Exp Ther Med*. 2020;19:2733-2740.
17. Yang L, Yu Y, Yu X, et al. Downregulated expression of hsa_circ_0005556 in gastric cancer and its clinical significance. *Dis Markers*. 2019;2019: 2624586.
18. Lin J, Cai D, Li W, et al. Plasma circular RNA panel acts as a novel diagnostic biomarker for colorectal cancer. *Clin Biochem*. 2019;74:60-68.
19. Fox JG, Wang TC. Inflammation, atrophy, and gastric cancer. *J Clin Invest*. 2007;117: 60-69.
20. Correa P. Helicobacter pylori and gastric carcinogenesis. *Am J Surg Pathol*. 1995;19 Suppl 1:37-43.
21. Jeuck TLA, Wittekind C. Gastric carcinoma: stage migration by immunohistochemically detected lymph node micrometastases. *Gastric Cancer*. 2015;18:100-108.
22. Wei J, Wu N, Liu B. Regional but fatal: Intraperitoneal metastasis in gastric cancer. *World J Gastroenterol*. 2016;22:7478-7485.
23. Tang Q, Hann SS. Biological roles and mechanisms of circular RNA in human cancers. *Onco Targets Ther*. 2020;13:2067-2092.
24. Wu J, Qi X, Liu L, et al. Emerging epigenetic regulation of circular RNAs in human cancer. *Mol Ther Nucleic Acids*. 2019;16:589-596.
25. Li T, Shao Y, Fu L, et al. Plasma circular RNA profiling of patients with gastric cancer and their droplet digital RT-PCR detection. *J Mol Med (Berl)*. 2018;96:85-96.
26. Nilsson RJS, Balaj L, Hulleman E, et al. Blood platelets contain tumor-derived RNA biomarkers. *Blood*. 2011;118:3680-3683.
27. Linde ME, Mijnc JC, Pham TV, et al. Evaluation of potential circulating biomarkers for prediction of response to chemoradiation in patients with glioblastoma. *J Neurooncol*. 2016;129:221-230.
28. Chen S, Li T, Zhao Q, et al. Using circular RNA hsa_circ_0000190 as a new biomarker in the diagnosis of gastric cancer. *Clin Chim Acta*. 2017;466:167-171.
29. Li J, Sun D, Pu W, et al. Circular RNAs in cancer: Biogenesis, function, and clinical significance. *Trends Cancer*. 2020;6:319-336.
30. Pan J, Zhang F, Sun C, et al. miR-134: A human cancer suppressor? *Mol Ther Nucleic Acids*. 2017;6:140-149.
31. Qu J, Yang J, Chen M, et al. CircFLNA acts as a sponge of miR-646 to facilitate the proliferation, metastasis, glycolysis, and apoptosis inhibition of gastric cancer by targeting PFKFB2. *Cancer Manag Res*. 2020;12:8093-8103.
32. Li H, Shan C, Wang J, et al. CircRNA hsa_circ_0001017 inhibited gastric cancer progression via acting as a sponge of miR-197. *Dig Dis Sci*. 2021;66:2261-2271.

Publisher's Note Springer Nature remains neutral with regard to jurisdictional claims in published maps and institutional affiliations.